REVIEW

QSAR AND 3D-QSAR IN TIMIŞOARA. 1972–2005

Adrian CHIRIAC,[a] Dan CIUBOTARIU,[b] Simona FUNAR-TIMOFEI,[c] Ludovic KURUNCZI,[b] Maria MRACEC,[c] Mircea MRACEC,[c] Zoltan SZABADAI,[b] Edward ŞECLĂMAN[b] and Zeno SIMON[c*]

[a] West University, Timişoara, Faculty of Chemistry-Biology-Geography, 16 Pestalozzi, 300115, Timişoara, Roumania
[b] "Victor Babeş" University of Medicine and Pharmacy, Timişoara, 2 Eftimie Murgu, 300041, Timişoara, Roumania
[c] Institute of Chemistry "Coriolan Drăgulescu" of the Roumanian Academy, 24 Mihai Viteazul, 300223, Timişoara, Roumania

Received July 15, 2005

This is a review on studies in QSAR and 3D-QSAR performed by the QSAR-group of Timişoara over a period of more than thirty years. The main interest of our group was the inclusion of molecular stereochemistry in QSAR. The main contributions are the minimal steric difference MSD and the minimal steric topologic difference MTD methods, introducing of new molecular shape descriptors and of new topologic indices. Among them, the MTD method is considered as a precursor of modern 3D-QSAR. The main QSAR applications are also described – the most important QSPR-type studies for dye–cellulose fibre interactions. Contribution to, and especially applications of several modern techniques, such as CoMFA, neural networks, ligand-receptor docking and interactions, classifications in large data bases are also described.

INTRODUCTION

Interests in QSAR appeared in Timişoara soon after publication in 1964 of the first JACS QSAR paper of Hansch.[1] It was the late R. Vâlceanu, at the Chemical Research Centre of the Roumanian Academy in Timişoara, who founded an informal group for studies in Quantitative Structure-Biological Activity Relations. A. Chiriac, then doctoral fellow of Vâlceanu, Z. Szabaday and Z. Simon were the first members of this group. The first paper[2,3] was published in 1972 and used the MLR technique of Hansch. Interest in QSAR appeared at about the same time also in other groups in Roumania at the Chemico-Pharmaceutical Research Institute (ICCF) in Bucharest and at the Organic Chemistry Department of the "Babeş-Bolyai" University in Cluj which published also the first Roumanian QSAR book.[4]

In the early 70s, classical Hansch QSAR proved quite successfull with hydrofobicity and substituent reactivity as structural variables, but description of molecular stereochemistry was given, at the best, by rather artificially introduced indicator variables. The description of molecular stereochemistry for QSAR became main item for the Timişoara QSAR-group. QSAR studies were soon performed also at the Chemistry Departments of the University, of the Polytechnical Institute and at the Biophysics Department of the Medicinal Institute – all in Timişoara. Until 1990 only Roumanian computational technique was available to our group. Thereafter several modern computers and drug design programs become available, largely due to M. Bohl (then at TRIPOS, Germany) and to T. I. Oprea (then at ASTRA ZENECA, Sweden).

MINIMAL STERIC DIFFERENCE (MSD)

Let us consider a series for the QSAR of N molecules (ligands), L_i, i = 1,2,..., N. The idea of MSD is that each potential ligand L_i should fit at the best into the binding site of the receptor and that, the larger the ligand-binding site misfit, the lower the affinity (the biologic activity Y_i)[5] – Fisher's old "key-into-lock" idea.[6] The molecules are superposed, atom per atom, upon the "standard", L_0, the natural effector or the

* Corresponding author: zsimon@acad-icht.tm.edu.ro

molecule (from the QSAR series) with the highest activity, which is supposed to fit perfectly the binding site. For molecule L_i, one counts the non-superposable atoms and this is MSD_i.

In the superposition process the L_i molecules are oriented according to a common molecular core or according to overlapping of the "pharmacophore atoms". If a molecule has several low energy conformations one retains the one with maximal superposition upon L_0 (lowest MSD). In the superposition process, the small atoms are neglected, as well as small differences (0.5 Å) between bond lengths and bond angles. The superposition procedure is the one the organic chemist would adopt; it depends strongly on chemical intuition. There may appear biases, especially if different condensed cycles are to be superposed. Sometimes, for the more voluminous third and higher period atoms, 1.5 or 2 units are considered, instead of 1, for second period atoms. The superposition procedure of the MSD method is certainly more realistic for ligand-receptor interactions than the previous procedures of Amoore[7] or Allinger[8], based upon superposition of molecular gravity centers and main axis. Details for the superposition procedure can be found in[9].

The superposition procedure gives rise to a network, the hypermolecule, $\hat{H}$, with M vertices (j = 1,2,...,M) corresponding to approximate atomic positions and edges corresponding to valence bonds between atoms. The hypermolecule can be considered also as a molecular graph, with all the topological consequences. Each molecule L_i can be described by a "vector" with M components, x_{ij} (x_{ij} = 1 if vertex j is occupied in L_i and 0 if not), or by k such "vectors", characterized by x_{ijk}, if there is more than one conformation (k) considered. Further details can be found in [10] (chap 3).

As an example, the superposition of some L and D-amino acidic side chains is illustrated in Fig. 1, together with the corresponding hypermolecule with M = 8 vertices. As an example, the L-Phe side chain, considered as standard, L_0, occupies vertices j: 2-8; the one of D-Ala j: 1; the one of L-His j: 2-5,7,8. For L-cyclohexyl-Ala, the cyclohexyl ring, in chair conformation, is considered superposable upon the phenyl ring.

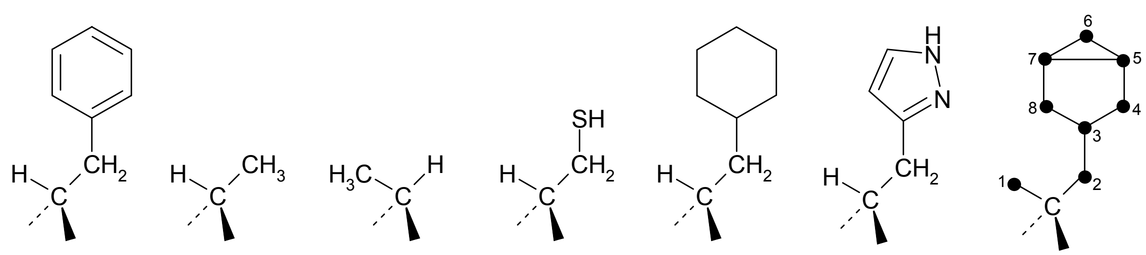

L-Phe	L-Ala	D-Ala	L-Cys	L-cC_6H_{11}-Ala	L-His	$\hat{H}$
MSD = 0	6	8	5(4,5)	0	1	

Fig. 1 – Superposition and MSD values for some amino acidic side chains and hypermolecule; L-Phe as standard L_0. For MSD of L-Cys, value in parenthesis (4,5) for the SH-group as 3rd period atom, considered with a relative 1.5 volume value.

In the first publised MSD-paper,[5] MSD-biologic activity correlation was applied to a series of N = 42 amino acidic substitution derivatives of oxytocine, with the decrease of biologic activity (on a logarithmic scale) produced by aminoacidic substitutions as Y. The correlational result, r^2 = 0.56 is statistically significant and similar to the result obtained correlating the same Y-values with variations, produced by amino acidic substitution, in 6 intermolecular force types (hydrophobicity, aromatic character, electric charge at pH = 7, etc).[3] For a series of N = 14 hydrolysis rates of amino acidic esters catalyzed by α-chymotrypsine r^2 = 0.83 is obtained with MSD (r^2 = 0.64 with hydrophobic increments), but only r^2 = 0.02 for a series of N = 20 adenosinkinase catalyzed ATP phosphorylation rates of β-ribosides of nitrogen bases.[5] For some other examples of MLR correlations with MTD and other structural variables see the Examples – paragraph of this review. Most, but not all results are statistically significant.

The rather limited success of the simple MSD-method is not surprising. It is unlikely to have the receptor binding site as a perfectly complementary replica of the standard L_0, even if this is the natural effector and that all supplementary (with respect to L_0) atoms of the L_i-molecules should produce detrimental effects. Some of these atoms could be in the exterior, aqueous solution, without influence upon the receptor affinity.

As example for all MSD and MTD variants, we list in Table 1 molecular structures, structural parameters and Y-values for the acetylcholine (AChE) catalyzed hydrolysis rates of N = 25 acetic acid esters (CH_3COOR). The biological activities Y are logarithms of second order rates, as studied by Järv et al[11]. The corresponding hypermolecule[12] is depicted in Fig. 2. The MSD values with respect to acetylcholine, the natural substrat of AchE, are also added to Tab. 1.

Table 1

CH_3COOR hydrolysis rates catalyzed by AChE

i	R	Y	σ	π	E_S	MSD	$j(x_{ijk}=1)$
1	C_6H_5	6.72	0.60	2.13	0.38	4	2-6
2	$CH_2CH_2CMe_3$	6.30	0.00	2.98	0.40	0	4-8
3	CH_2CH_2SEt	5.40	0.22	1.95	0.44	3	5-7,9
4	CH_2SEt	5.35	0.56	1.45	0.44	2	5-7;4-6;5,6,8
5	$CH_2CH_2CHMe_2$	5.32	0.00	2.30	0.43	1	4-7;4-6,8;5-8
6	$CH_2CH_2NO_2$	5.20	0.62	1.31	0.40	1	4-7;4-6,8;5-8
7	CH_2CH_2Cl	5.02	0.39	1.39	0.48	3	5,6;6,10
8	$CH_2C{\equiv}CH$	4.81	0.55	0.94	0.60	5	6,11
9	nC_5H_{11}	4.74	0.00	2.50	0.40	3	5-7,9
10	nC_7H_{11}	4.75	0.00	3.50	0.40	5	5-7;9,12,13
11	$(CH_2)_4SEt$	4.73	0.03	2.95	0.40	5	5-7,9,12,13
12	cC_6H_{11}	4.71	0.00	2.51	0.98	4	2-6
13	nC_4H_9	4.72	0.00	2.00	0.40	2	4-6;5,6,8;5-7
14	nC_6H_{13}	4.68	0.00	3.00	0.40	4	5-7,9,12
15	$(CH_2)_3SEt$	4.67	0.08	2.45	0.40	4	5-7,9,12
16	$CH_2C_6H_5$	4.66	0.25	2.26	0.38	5	5-7,10,14,15
17	CH_2CHMe_2	4.32	0.00	1.80	0.35	4	5,6,10
18	$CH_2CH{=}CH_2$	4.10	0.23	1.23	0.23	3	5,6;6,10
19	nC_3H_7	3.91	0.00	1.50	0.39	3	5,6;6,10
20	CHMeEt	3.69	0.00	1.86	0.93	4	1,5,6;2,5,6
21	C_2H_5	3.36	0.00	1.00	0.36	4	6;2
22	CH_3	3.00	0.20	0.50	0.07	5	-
23	$CHMe_2$	2.72	0.00	1.30	0.93	5	2,6;1,2
24	CMe_3	1.30	0.00	1.98	1.74	6	1,2,6
25	CMe_2Et	1.30	0.00	2.48	1.74	5	1,2,5,6;1-3,6

Y = log (k_{cat}/K_M) according to[11]; σ* – Taft constants; π – Hansch hydrophobicities, E_S – steric constants, all quoted by Järv[11], $j(x_{ijk} = 1)$, vertices occupied in the hypermolecule of Fig. 2. Where several conformations for one molecule are listed, the first is used for MSD calculations. The standard, acetylcholine ($CH_3COOCH_2CH_2NMe_3^+$) occupies vertices j:4-8; AChE – acetylcholinesterase.

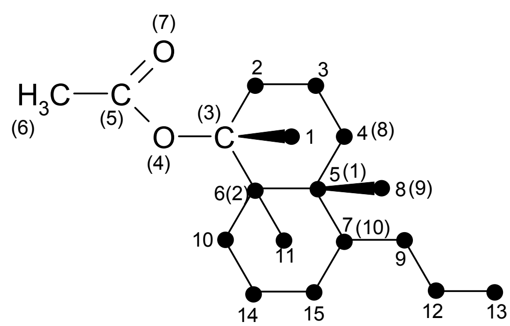

Fig. 2 – Hypermolecule and vertex j numerotation[12] for the acetic acid ester series of Table 1. Numbers in parenthesis, numerotation of acetylcholine atoms in the complex with AChE, according to the X-ray crystallography data[13].

The results for the MLR-correlation with σ*, π and E_S are[12]:

$$\hat{Y} = 3.111 + 3.0110\sigma^* + 0.968\pi - 1.935E_S; \quad r^2 = 0.779, \quad r^2_{CV} = 0.658(0.571) \tag{1}$$

Introduction of MSD improves the statistical results:

$$\hat{Y} = 3.903 + 2.914\sigma^* + 0.906\pi - 1.548E_S + 0.249MSD; \quad r^2 = 0.849, \quad r^2_{CV} = 0.726 \tag{2}$$

Crossvalidational results are on a leave one out basis; the result in parenthesis in on an ODD/EVEN basis (see next paragraph).

MINIMAL STERIC/TOPOLOGIC DIFFERENCE (MTD)

The M vertices j of the hypermolecule $\hat{H}$ can be situated within three different regions with respect to the receptor binding site: interior of the cavity site-characterized by $\varepsilon_j = -1$, within the cavity walls – characterized by $\varepsilon_j = +1$ and in the exterior aqueous solution – characterized by $\varepsilon_j = 0$. Atoms occupying cavity vertices are expected to have a beneficial effect on the ligand-receptor affinity, atoms occupying wall vertices – a detrimental effect, atoms occupying exterior vertices – to be irrelevant for the affinity.[14] The correlational equation is of the type:

$$\hat{Y}_i = a_0 + a_1\sigma_{1i} + ... + \beta_i MTD_i \, ; \quad i=1,2,...,N \tag{3}$$

with σ_{1i},... – other structural parameters characterizing molecule L_i and MTD_i its minimal steric difference – the number of occupied wall vertices plus the number of unoccupied cavity vertices:

$$MTD_i = s + \sum_j \varepsilon_j x_{ij} \, ; \quad j=1,2,...,M \tag{4}$$

Here s is the total number of cavity vertices.

The ε_j – parameters, characterizing the three types of vertices are determined by an optimization procedure. One begins with an initial attribution of ε_j^0-values, characterizing the "start map" S_0, often the L_0 standard of MSD or obtained by trial and error. The ε_j^0-parameters are changed one by one, and the monosubstituted map which yields the best correlation with eqs (3) and (4) is used for the next ε_j-monosubstitution cycle. The optimization ends when the maximal correlation coefficient r for the $Y - \hat{Y}$ correlation is obtained. The resulted ε_j-attributions represent the optimized receptor map, S*, and should give an idea for the shape of the receptor cavity. For further details concerning MTD see[15] and[10] (chap. 3).

The MTD-method has also a series of drawbacks. The construction of the hypermolecule is, sometimes, ambiguous. For different start maps, different optimized map, S*, are often obtained.[16] Also if within the series for QSAR, a group of 2 vertices (a,b) are either unoccupied or both occupied by the L_i-molecules, the attributions ε_a=ε_b=0; ε_a= -1, ε_b= +1; ε_a= +1, ε_b= -1 yield identical correlational results.

Among the first MTD-QSAR studies is the one of Bădilescu and Simon[17] for the affinity of N = 49 haptenes, mostly pyridine and succinylanilide derivatives against an antibody elicited by 3-azopyridine coupled to ovalbunine. With MTD, π and δ = 1 for the presence of an atom with lone electron pair in a certain position r^2 = 0.78 results. Another MTD-QSAR[18] with MTD and π for dihydorfolatereductase inhibition by N = 15 pyrimidine derivatives (alkyl, cycloalkyl, naphtyl as 5 substituents) r^2 = 0.96 is obtained; for the Y-π correlation r^2 = 0.59. The optimized receptor map compares favorably with some results of Silipo and Hansch[19], by MLR, for a more extended series of triazine derivatives.

Reliability of MTD results.[10] The MTD-QSAR implies a rather large number, M of adjustable ε_j-parameters; often M > N. Following procedure is generally adopted: the N molecules of the series for QSAR are listed in decreasing order of Y-activities. The odd numbered molecules (i:1,3,5,...) are considered as a learning set, the even numbered (i:2,4,6,...)as test set; from the even numbered L_i's, those being the single occupants of a certain j-vertex are transferred to the learning set. The receptor map and correlational equation for the learning set are used to calculate the $\hat{Y}$-activities for the test series; the $Y - \hat{Y}$ correlation for the test set is used to obtain an r^2_{CV}. This should be a more realistic approximation for the predictive power of the MTD-method. We call this the ODD/EVEN selection.

Multiple low energy conformations.[12] If some L_i molecules have more than one low energy conformation, its minimal steric difference will be:

$$MTD_i = \underset{k}{Min}(s + \sum_j \varepsilon_j x_{ij} k) \, ; \quad j:1,2,...,M; \quad k=1,2,... \tag{5}$$

The conformation, k, which yields the lowest MTD-value (*i.e.*, the one which fits best the receptor) is selected.

Problems related to the selection of conformations and their relative energies were first discussed in a QSAR on a series of phenyl and indolylacetic acid derivatives with auxinic activity.[20] By hand calculations of repulsions (via 6-12 Lenard-Jones potentials) were also performed for some key conformations.

After 1990, with access to computational molecular mechanics techniques, the statistical weights of various conformers were also considered.[21] If several conformations are available for L_i and only one is biologically active, the actual concentration of this active conformer is lower than the one of L_i, the Y_i^{adj} activity higher than the experimental, Y_i for the mixture of all conformers of L_i:

$$Y_i^{adj} = Y_i - \log \alpha_i\,; \quad \alpha_i = \frac{e^{-U_a/kt}}{\sum_k g_k e^{-U_k/kT}} \tag{6}$$

U_a and U_k are internal energy of the active and other conformations, g_a and g_k statistical weights (of isoenergetic conformers). This is the MTD-adj method.[21]

For the series of N=25 acetic esters in AChE catalyzed hydrolysis rates of Table 1, the hypermolecule has M = 15 vertices and some molecules have up to 3 conformations. The $\hat{H}$ was constructed with a minimal number of vertices, so that it includes at least one conformation for each molecule. The optimized receptor map is depicted in Fig. 3, the correlational equation (r_{CV}^2 on an ODD/EVEN - basis):[12]

$$\hat{Y} = 8.434 + 1.683\sigma * -0.753\text{MTD}; \quad r^2 = 0.867, \quad r_{CV}^2 = 0.661 \tag{7}$$

Fig. 3 – Optimized receptor map of AChE catalyzed CH_3COOR-hydrolyses (see Table 1)[12]. Vertex j attribution, o-cavity vertices; ● wall vertices; • exterior, irrelevant vertices. Common core vertices (atoms) are not numbered (as j).

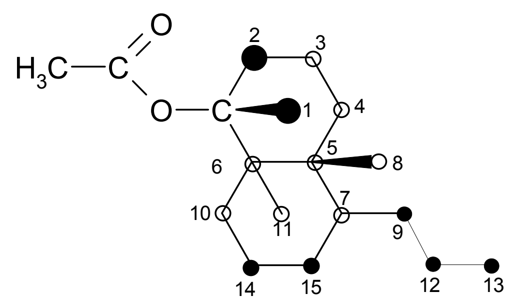

In the QSAR with the MTD-adj method for the same series, a more complete investigation of low energy conformations using molecular mechanics techniques gives a $\hat{H}$ with a total of M = 64 vertices. The receptor map has an increased number of cavity and wall vertices, with most cavity vertices concentrated in the region occupied by the acetylcholine molecule. The correlational equation is (r_{CV}^2 on an ODD/EVEN-basis):[21]

$$\hat{Y} = 12.913 + 2.956\sigma^* - 0.878\text{MTD}; \quad r^2 = 0.966, \quad r_{CV}^2 = 0.810 \tag{8}$$

The SIBIS and HIBIS methods. Topologic restrictions in receptor map optimization. Some interesting variants of the MTD method which prefigurate the MTD-PLS receptors mapping were developed by Motoc and Dragomir-Filimonescu, the SIBIS and the HIBIS-methods.[22-24] Cavity and wall vertices are considered separately in these methods. In SIBIS, atoms or groups occupying a j vertex are described by a steric k_p parameter introduced by Anstel et al[25] (*i.e.*, $x_{ij}=k_p$ – if occupied, 0 – if not) in HIBIS – by Recker hydrophobic fragmental constants.[26] Separate steric differences are calculated for cavity and wall vertices. In SIBIS:

$$SD_{c,i}^* = \sum_{j(c)} x_{ij}; \qquad SD_{w,i}^* = \sum_{j(w)} x_{ij}; \qquad \hat{Y}_i = a_s + b_s SD_{c,i}^* + c_s SD_{w,i}^* \tag{9}$$

i.e., summation is performed over the cavity and respectively wall vertices. In HIBIS:

$$f_i = \sum_{j(c,v)} x_{ij}; \qquad \hat{Y}_i = a_H + b_H f_i + c_H f_i^2 \tag{10}$$

the summation is performed over both cavity and receptor walls.

In the receptor map optimization procedure of SIBIS and HIBIS, two topological restrictions are introduced. First – the j-cavity vertices of the receptor map should form (via edges in $\hat{H}$) a single connected graph. Second – the exterior (irrelevant) vertices j should also form a single connected graph; prior to optimization, the j vertices "suspected" to be exterior are connected, by virtual edges, to a common, virtual exterior vertex.[22] A result of these topological restrictions is an improved "stability" of the optimization process – the same optimized receptor map for different start maps.[24]

This first topologic restriction was adopted also in some MTD papers:[27,28] the (nonnumeroted) vertices of the common molecular core and the cavity vertices are forced to form a single connected graph. This corresponds to a unique, nonfragmented receptor cavity – a reasonable assumption. The second condition seems too restrictive: only marginal groups of the molecules (and the corresponding j-vertices) will be into the exterior, outside the receptor, it is unlikely to have them connected.[28] Some comparative MTD studies with different topological restrictions were performed for a series of cardiotoxic bufadienolides and cardenolides which were divided into a learning set of N=30 steroids and a test set of N=16 steroids.[22,29] The receptor map and correlational equation for the learning set were constructed in three different ways. First, only the connectivity restriction for cavity and common core vertices was used and from equivalent (as r^2) optimized receptor map, the one with a minimal number of cavity and wall vertices was selected;[27] r^2=0.72 was obtained for the learning set, $r^2_{CV} = 0.63$ for the test set. In a second MTD study without connectivity restrictions, five different start receptor maps produced five different optimized receptor maps;[29] for the receptor map r^2 = 0.84 was obtained for the learning set, but only $r^2_{CV} = 0.40$ for the test set. In a third SIBIS study both connectivity restrictions were used but, from a total of M=24 (non-common core) vertices, only 6 (j:2,3,8-10,16) were connected to a virtual exterior vertex[22,29]; for the learning set, r^2 = 0.67 was obtained but only $r^2_{CV} = 0.10$ for the test set.[28] Thus, the optimization with a single connectivity restriction (cavity + common vertices) yields the best results for the test set.

Other optimized receptor maps, which respect the connectivity restriction for cavity + common vertices are depicted in Fig. 2 and Fig. 7, while the optimized map of Fig. 6 does not respect this restriction.

RECEPTOR SITE MAPPING. MTD-PLS

Mapping of receptor sites is a "dream" for QSAR and 3D-QSAR, probably also, as intention of the creators of CoMFA.[30] There is a difficulty: in any QSAR approach, a certain (difficult to define) quantity of pertinent information is introduced by molecular structure parameters and especially by the biologic activities, Y_i, of the N molecules considered. This information seems to be proportional to N-1. To describe the receptor site, various parameters such as atomic electric charges, van der Waals and hydrogen bonding characteristics, local deformabilities should be given for the dozen of atoms of the receptor site. According to Topliss[31,32] in order to avoid chance correlation, in MLR-QSAR, the number N of Y_i's should be at least 3-4 times larger than the number M of structural parameters to be characterized. This seems to be a result of some principle of constancy of pertinent input to output information and is certainly true for any QSAR-type procedure, including CoMFA.[33]

The basic idea of the MTD-PLS procedure[34] was to characterize atoms occupying the vertices of the hypermolecule by parameters characterizing an as realistic as possible force field,[35] inspired by scoring functions used to calculate ligand receptor affinities.[36] Supplementary input information is introduced by some chemical intuition based restraints: steric misfit is always detrimental, hydrophobic interactions-beneficial (the receptor site is, usually, much less polar than the surrounding water). Due to the large number of structural parameters (number M of vertices multiplied by the times number of intermolecular force types considered), a PLS technique had to be used.

As precursor of the MTD-PLS approach the work of Palyulin *et al.*[37] is to be considered; they characterized atoms occupying hypermolecule vertices, j, by different parameters used in other types of QSAR, but these cannot be consistently related to a realistic force field. Also, the SIBIS and HIBIS methods of Motoc *et al.*[22,23] use steric Anstel parameters, respectively Rekker fragmental hydrophobicities to characterized atoms occupying j's and impose graph theory-based restrictions on the optimization procedure used in obtaining the correlational equation.

The correlational equation used for MTD-PLS is of the type

$$\hat{Y}_i = a_0 + \sum_{j=1}^{n}(a_{jV}V_{ij} + a_{jH}H_{ij} + a_{jp}P_{ij} + a_{jS}S_{ij} + a_{jA}A_{ij} + a_{jD}D_{ij}) \quad (11)$$

Here, V_{ij}, is the fragmental van der Waals volume of the atom (XH_n-group) occupying vertex j in molecule i, H_{ij} the fragmental hydrophobicity of the same atom, P_{ij} the polarisability (van der Waals atraction is proportional to the product of polarisabilities of atoms), S_{ij} – the electric charge (as resulted from the quantum chemical calculation included in modern molecular mechanics programs);[40] A_{ij} and D_{ij} – parameters characterizing proton acceptor, respectively donor tendencies in hydrogen bonding.

Applied to a series of N = 69 dioxin analogs and polyhalogenated biphenyls,[34] the first PLS model with 105 descriptors (less than the theoretical 6 × 21; no atoms with hydrogen bonding abilities are included), yields $r_Y^2 = 0.728$, $q^2 = 0.553$ for correlation with AHH-activity (induction of aryl hydrocarbon hydroxylase). The final PLS-model, with 43 molecules and 52 descriptors yields $r_Y^2 = 0.819$, $q^2 = 0.732$. The attribution of beneficial or detrimental character to atoms and vertices is in good agreement with vertex attribution by MTD to the same series (59 chlorinated-only, derivatives); for this MTD study,[38] $r^2 = 0.699$, $r_{CV}^2 = 0.728$. Nevertheless, in this study, there appear also positive a_{jV} –coefficients (beneficial steric misfit!) or negative a_{jH} –potential (detrimental hydrophobic interactions!).

In order to have steric interactions always detrimental, hydrophobic and polarisation-favored interactions always beneficial, following restraints were introduced for the “correlation coefficients” of eq. (11):

$$a_{jV} \le 0; \quad a_{jH} \ge 0; \quad a_{jP} \ge 0 \quad (12)$$

The colums of variables for which the $a_{j\mu}$-coefficients do not satisfy conditions (12) are simply eliminated and, hereby, some pertinent input is introduced in the MTD-PLS approach.[39]

This MTD-PLS approach was applied to the AChE catalyzed CH_3COOR hydrolysis rates of Table 1 (Chap. 3). This first MTD-PLS model with all N = 25 molecules and 49 structural variables (electric charges of atoms of the common CH_3COO moiety were also introduced) yields $r_Y^2 = 0.835$, $q^2 = 0.597$, while for the final model with N = 22 molecules and 41 variables (V_{ij}, H_{ij}, S_{ij}) - $r_Y^2 = 0.949$, $q^2 = 0.796$.

The $a_{j\mu}$-coefficients of the corresponding type (11) equation were compared with X-ray crystallography data for the AChE-acetylcholine complex.[13] Results are given in Table 2. The carbonylic atom >C= (5) is at 3 Å from one imidazolic N-atom of His from the catalytic AChE – site. According to an AM1 calculation,[40] this N-atom has a partial charge of -0.191e; $a_{jS} = -30.65e$ requires, for a coulombian potential created by an receptor atom at 3 Å distance a partial charge of -0.39e for this atom. The negative a_{jV} values for j=1,2,6 are explained by the only 2.8 Å distance of $–CH_2-$ (j=6) to a receptor atom and, for vertices j:1 and 2 by their protrusion into the wall of the receptor gorge. The three CH_3 groups of $–N(CH_3)_3^+$ are in several contacts (at van der Waals distances) to the Phe,[330] His[440] and Trp[84] aromatic side chains which explains the significant, positive, a_{jP} – coefficients for j: 4,7 and 8. The CH_3-group in j:7 is in contact with the OE 1 atom of the Glu[194] side chain (negatively charged at pH 7), which explains the negative a_{7S}=-0.70 coefficient. Other $a_{j\mu}$ – coefficients are also at least nonconflicting with expectations for contacts with the AChE site for vertices not occupied by acetylcholine.[39] Some pertinent $a_{j\mu}$-values and ligand-receptor atoms are given in Table 2.

The final PLS-model has a total of 13 vertices and M = 43 structural variables, with N = 22 biologic activity (Y) data. There are a total of 39 × 3 = 117 type eq. (12) restrictive conditions which eliminate 15 columns of structural parameters. The input/output quotient is certainly not enough to satisfy the Topless conditions[31] concerning chance correlation, but comparison of the $a_{j\mu}$-coefficients with X-ray crystallography contacts is encouraging.

The MTD-PLS method with restrictive conditions (12) was applied also to a series of N = 49 estrogen derivatives with agonistic activity.[41] The hypermolecule has 35 vertices. For the initial PLS-model (99 descriptors) $r_Y^2 = 0.808$, $q^2 = 0.369$. The final PLS model, based upon only N = 19 molecules (27 descriptors) is statistically satisfactory: $r_Y^2 = 0.942$, $q^2 = 0.757$. The main results, concerning $a_{j\mu}$ values – steric misfit for the steroidic position 2, benefic hydrophobic and polarisability enhanced van der Waals interactions for 17α-CH=CH-X groups are confirmed by ligand-receptor contacts based on X-ray crystallography, even the first, statistically weak, PLS model yields $a_{j\mu}$-results consistent with X-ray crystallography for position with a sufficient high variability in substituents.

Table 2

Comparison of $a_{j\mu}$ coefficients[39] with X ray crystallography data for the AChE-acetylcholine complex[13]. Final PLS-model[39]

Atom	**r (nr)**	**$a_{j\mu}$**				**AChE-acetylcholine contacts**
		μ=S	**V**	**P**	**H**	
$-CH_3$	(6)	1.84	-	-	-	
-O-	(4)	-1.05	-	-	-	
>C=	(5)	-30.65	-	-	-	3 Å from N(imidazole)His catalytic site
=O	(7)	23.72	-	-	-	
$-CH_3$	4 (8)	0.05	-	0.075	0.293	All three CH_3 groups in numerous contacts with hydrophobic aromatic side chains of Phe[330], His[440], Trp[84]
$-CH_3$	8 (9)	6.56	-	0.067	0.443	Contact to OE1 (negative charge) of Glu[199]
$-CH_3$	7 (10)	-0.70	-	0.042	0.149	
	5 (1)	0.24	-	0.029	-	
$-CH_2$	6 (2)	0.40	-0.031	-0.023	-	2.8 Å to CD2-His[440]
	1	-12.68	-0.017	-0.067	-	The CH_2CH_2 –moiety of acetylcholine is in a narrow gorge of AchE; vertices j = 1,2 penetrate the walls of this gorge
	2	-10.40	-10.40	-0.058	-	

MOLECULAR SHAPE DESCRIPTORS

Steric parameters in QSAR like those introduced by Charton, Taft, Verloop and Hogenstraten should be related to the shape of molecules or substituents. In order to study their physical significance one is interested in the geometric characteristics of the corresponding substituents – described as envelopes of the component atoms described by hard spheres of van der Waals radii. These characteristics are van der Waals volumes and surfaces (V^W, S^W) and synthetic shape indicators, some with vectorial characteristics – termed also as molecular van der Waals space. They are interesting also in relation to the physical significance of topologic indices.[42]

Molecular volumes and surfaces by Monte Carlo method.[43,44] The space occupied by a molecule can be described, in the approximation of hard spheres as follows: each atom j of molecule L is represented by an isotropic sphere, centrated at x_j, y_j, z_j with the van der Waals radius, r_j^W. The points (x,y,z) within the interior of the molecular envelope satisfy at least one of the condition:

$$(x_j - x)^2 + (x_j - y)^2 + (x_j - z)^2 \le (r_j^W)^2, \quad j{:}1, 2, \ldots m \tag{13}$$

with m, the number of atoms within L. The molecule L is within paralelipipedium of volume V_P. By a Monte Carlo technique, a number n_T of points are generated within the paralelipipedium, n of them satisfy at least one condition (13), *i.e.* – they are within the interior of L. The van der Waals volume of L will thus be:

$$V_L^W = \frac{n}{n_T} V_P \tag{14}$$

In order to calculate envelope surfaces, a total of n_T points are generated on the surface of each atom j *via* randomly generated polar θ, φ coordinates. Of these, n_{ej} –points are contained in neither of the other atomic spheres of L (*i.e.*, – satisfy neither of the m type 13 conditions). The van der Waals surface, S_L^W is calculated as:[45]

$$S_j^W = \frac{n_{ef}}{n_T} 4\pi (r_j^W)^2; \qquad S_L^W = \sum_j S_j^W; \quad j = 1, 2, \ldots, m \tag{15}$$

Direct volume and surface calculation, by tridimensional geometry, for envelopes of interesting hard spheres is cumbersome, which makes the Monte-Carlo calculations a much easier way; their reliability has been assessed by comparing results with other, more conventional, calculations.[44]

A Monte Carlo method was used also in modeling and simulation of copolymerization reactions[46].

MCD-version of MSD.[47] MSD between two molecules was calculated also as the minimal nonoverlapping van der Waals envelope volumes *via* the Monte Carlo method, using type (13) condition to determine the appartenance of random points to the nonoverlapping envelopes. With n_I – the number of such points:

$$MCD = V_P \frac{n_I}{n_T} \tag{16}$$

Molecular superposition, etc, is the same as for the simple MSD-method. As an application, let us mention the correlation of affinity for an anti-(p,p'-azophenylazo)benzoate antibody of N = 11 substituted benzoic acid derivatives.[47] The highest affinity molecule, 4-Cl-benzoat was used as standard. The affinity MCD – correlation yields r^2=0.46.

Synthetic shape indicators were developed, on hand of van der Waals envelopes, with the aim to analyze the difficulties related to the quantitative estimation of the molecular shape and of the effects in the QSAR and chemical reactivity.[48] By some principles of analytical geometry, for each substituent a rotational ellipsoid results, and the semiaxes (a, b, c) constitute a first set of shape indicators. Other shape indicators are obtained from the equivalent radii, $r(V^W)$ and $r(S^W)$, for the volume and respective area of the substituent's van der Waals envelope:

$$r(V^W) = \left(\frac{3V^W}{4\pi}\right)^{1/3} \quad ; \quad r(V^W) = \left(\frac{S^W}{4\pi}\right)^{1/2} \tag{17}$$

The quotient $V^W/S^W = R^{WV}$ can be used as a measure for the "spheric (globular) character" of the substituent – the smaller R^{WV} – the more near to sphericity the substituent. As example, for eclipsated n-Bu, R^{WV} = 0.716, for the intercalated conformer -0.705, the lowest value is for the t-Bu radical.

The rotational parameters δ, G were introduced in an attempt to quantify the vectorial nature of steric effects. G is here the maximal length of the substituent along the direction of the valence binding the substituent to the molecular core, δ – the radius of a cylinder with the volume equal to the substituent's V^W and the axis equal to G.

Charton-like parameters, υ'_V and υ'_S were defined for substituents as:

$$\upsilon'_V = r(V^W) - 1.2\,; \qquad \upsilon'_S = r(S^W) - 1.2 \tag{18}$$

and correlated with the corresponding υ-Charton parameters in order to test its physical significance. There is a satisfactory correlation only when substituents have a general spheric (tetrahedral) type of shape, but fail when substituents of different shapes are considered together. The empiric υ-Charton is related to a mean radius ($r(V^W)$, $r(S^W)$) only for substituents with a shape near to a tetrahedral symmetry. Several other correlations with these shape indicators and various empirical steric constants for substituents were also studied.[49-51]

Pattern recognition. A package of programs with theoretic-decisional and statistic methods, SARF, was constructed for QSAR, recognition of bioactive compounds and for other applications.[52] Pattern recognition were used in QSAR for quantification of topologic similarity. Two parameters were introduced, SDM and TSDM which quantify on a [0,1] scale the similarity, respectively dissimilarity, between molecules,[53] somewhat inspired by the concepts of MSD and hypermolecule. They were tested, with good results on the inhibition of microsomal aniline oxidation (*via* citocrome P450) by alcohols.[53] The SDM and TSDM can be used in setting up series for QSAR with a maximal dissimilarity between the considered molecules.[54]

Metric induced by minimal steric difference. According to Motoc,[55] MSD verifies the condition imposed for a dissimilarity index for metrics[56] in the context of QSAR, a results valid also for MTD and

MCD. MSD induces a Hausdorff space in the manifold M which describes (via hypermolecule) the steric structure of the molecules of the series for QSAR.

Topologic indices and their physical significance. New topologic indices were developed for structural quantification. Thus in order to differentiate heteroatoms, the van der Waals connectivity vA_i was used to define a Randić index $vA_i = A_i v_i$, with v_i the valence of the vertex within the graph, while $A_i = r_i^W, S_i^W, V_i^W$, *i.e.*, the van der Waals radius, surface or volume[57]. The reciprocal distance matrix:

$$RD = \left\{d_{j,l}^{-1}\right\}; \qquad j,l = 1, \ldots, n \tag{19}$$

with n-the total number of vertices for the molecular graph Γ, was used to introduce and generalize a series of nondegenerated indices. Such an index is μ_j, the local invariant of each vertex of Γ, defined as:

$$\mu_j = \sum_j d_{jl}^{-1}; \qquad j = \overline{1,n}; \qquad j \neq l \tag{20}$$

with d_{jl} – the topologic distance between vertices j and l, n – the total number of vertices in Γ, thus μ_I is a measure for the influence of all vertices upon vertex j from the graph Γ. This local invariant μ_j was used to obtain various ${}^h\delta$ -indices with a Randić type formula extended to the generalized molecular connectivities.[59-61] These indices were used in monoparametric correlations with molecular properties of alcanes (boiling temperatures, gas chromatographic retension indices, atomisation enthalpy, molar refraction) .[62] Very good results were obtained with ${}^2\delta$; r^2 in the range 0.976 – 0.989.

A total of 16 generalized indices for topological distances (GTD's) were developed which contain also the previously described ${}^h\delta$ and μ_j –indices. They were calculated for the 72 alkanes C_2 to C_9, for which van der Waals volumes, surfaces and some other molecular shape descriptors. They were used in correlations with various physical properties. Correlations between GTD's and molecular shape descriptors based upon the molecular van der Waals space were also studied in order to understand the physical significance of topologic descriptors. The obtained results suggest that topological distance indices could be considered as descriptors for the size of molecules.[58]

Introduction of the topologic molecular space (MTS) over the M molecules, which are associated with a complete set of topologic indices, allowed a unique characterization of the molecules by a distance index ${}^\lambda d$ connected to models of pattern recognition. The analysis of the structure of ${}^\lambda d$ allowed to obtain a general condition for nondegeneration.[57,59,61,63]

MORE RECENT DEVELOPMENTS IN 3D-QSAR AND DRUG DESIGN METHODOLOGY

Some QSAR studies using CoMFA were performed for series of symmetric and nonsymetric ureea derivatives used as inhibitors of HIV-protease.[64,65] CoMFA as well as neural network methods[67] were used in QSPR-type studies for dye-cellulose fiber affinities.

Methodological contributions to CoMFA were also proposed: the steric potential, usually considered as a 6-12 Lenard-Jones potential presents an unrealistically steep increase below van der Waals contact distances. In the real case steric misfit will be circumvented by deformation of torsional and bond angles.[35] A simple proportionality between steric repulsion energy and overlapping volume of ligand molecule (van der Waals envelope) and CoMFA probe atom was considered for this steric potential.[68] In a CoMFA study with this type of steric potential, correlational results were similar to those obtained with the usual (6-12) potential, while stability of results (with respect to the positioning the molecule into the CoMFA framework) were improved.[69]

Another recent field, developed by the group of Maria Mracec (collaboration with T.I. Oprea), is receptor ligand interaction in the active site of the receptor. The AUTODOCK 3.0.5 software was used to study the conformational flexibility and behaviors of a series of ligands for the D2 dopamine receptors which can interact with both receptor states (high and low affinity states). One class of ligands fulfill the features of a pharmacophore model (proposed by Stark) for partial agonist. A 3D-model for the dopamine receptor was constructed based on X-ray data for bovine rhodopsin chains. Derivatives of 2-methylamino chromans and indoles were docked at the agonist site of the D2 receptor. The results of the study indicate that although the shape and volume of the active site is large enough, only the (2R)-chroman conformer accomodates well in the receptor pocket and interacts by hydrogen bonds with Ser[144] and by saline bridge with Asp.[86] Features of a pharmacophore model for the second class of compounds was hereby identified.[70] This group developes also drug design technique based on classification and search in large databases, such as the concept of privilegiated structures (work in progress).

ACETYLCHOLINESTERASE INHIBITING PESTICIDES: ORGANOPHOSPHORUS AND PHENYL-METHYL-CARBAMATE DERIVATIVES

Organophosphorus pesticides and phenyl-methyl-carbamates (PX) act as acetylcholine esterase (AChE) inhibitors according to following sequence of reactions.[71,72]

$$\mathrm{PX + EOH} \rightleftharpoons \mathrm{RX{\cdot}EOH} \longrightarrow \mathrm{EOP + HX} \xrightarrow{H_2O} \mathrm{EOH + POH} \qquad (21)$$

The pesticide molecule forms initially an absorbtion complex with AChE, followed, after the separation of the reactive leaving group, as XH, of a bond with AChE (E). Eventually, inhibition of AChE is released by hydrolysis. For Schrader type compounds and phenyl-methyl-carbamate derivatives, the leaving group, X, is $-OR_3$ (the most reactive substiutuent) and the phenolic moiety, respectively:

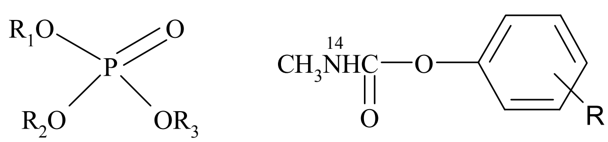

(22)

One of the first published QSAR paper of the Timişoara group[2] refers to a series opf N = 49 Schrader type compounds. Toxicity to mammals was correlated with 8 structural parameters (based on types of intermolecular forces); the MLR correlation with linear and quadratic terms yields $r^2 = 0.74$. A second attempt[73] extends the QSAR to a total of N = 71 molecules in a linear (only) correlation with the same parameters, to which MSD (standard-similar to acetylcholine) was added. An $r^2 = 0.50$ is obtained and a statistically significant correlation with a σ-Hammett type (reactivity) parameter for the leaving group, R_3.

Several other MLR-QSAR's were established with classical Hansch type parameters and MSD (different standards) for various series of organophosphorus compounds both as acetylcholinesterase and butyrylcholinesterase inhibitors.[74-77] Inhibitors of acetylcholinesterase are rather strongly dependent on steric parameters and also on electric charge if the P-atom charge distance is similar to the carboxyl C atom-N distance in acetylcholine. For example for a series of N = 60 derivatives of the general type $R_1R_2P(O)R_3$, with several positively charged R_3-leaving groups (respecting the above mentioned distance condition) the main correlational results are:[76]

$$\hat{Y} = 2.941 + 0.136\pi - 0.060\sigma^{\phi} - 0.028CT - 0.272MSD + 3.030EC\,; \quad r^2 = 0.77 \qquad (23)$$

The standard used for MSD calculations, similar to acetylcholine, is depicted in Fig. 4; the partial Y-MSD correlation, r = -0.707, is also statistically significant. Other structural parameters: π – Hansch hydrophobicities, σ^{ϕ} – Hammett type constant, CT – charge transfer character for R_3, EC – electric charge (R_3).

Fig. 4 – Standard for MSD for AChE inhibition by phosphorganic compounds.[76] Atoms bonded to free valences of L_0 are considered in commnon molecular core or in exterior solution and do not contribute to MSD.

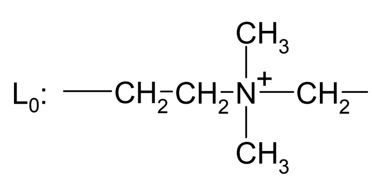

In short series of phosphoorganic derivatives, hydrophobicities and quantum chemical parameters yield sometimes good results, as well as MSD's calculated for rather unrelated standards, usually suggested by the most active molecule. Butyrylcholinesterase inhibition is more strongly dependent on hydrophobicity and the electric charge; for a series of N = 148 inhibitors, the best biparametric correlation ($r^2 = 0.76$) is the one with electric charge and reactivity (σ-Hammett) for the R_3 leaving group.[75,110] QSAR's were performed for a series of N = 25 amides of o-halogenoalkyl phosphates with various alkylic substituents at the O and N – atoms. The hypermolecule consists of M = 16 vertices. Molecular refraction, Kabachnik σ-constants and MTD were used as structural parameters. The best correlation, $r^2 = 0.82$, is due mainly to MTD.[108] The MTD method was applied also to map the site of acetyl cholinesterase phosphorylation for three series of phosphororganic derivatives:[109]

$$R_1R_2P(O)SCH_2CH_2N^+(CH_3)(R_3)\text{-}C_6H_4R_4; \quad N = 24 \tag{24}$$

$$R_1R_2P(O)SCH_2CH_2N^+(CH_3)(R_3)R_4; \quad N = 20 \tag{25}$$

$$R_1R_2P(O)SR_3; \quad N = 24 \tag{26}$$

The hypermolecule and receptor maps for the first two series are depicted in Fig. 5. With MTD and an indicator variable for positively charged N-atom (for first two series) correlational results between $r^2 = 0.71$ and $r^2 = 0.96$ are obtained.

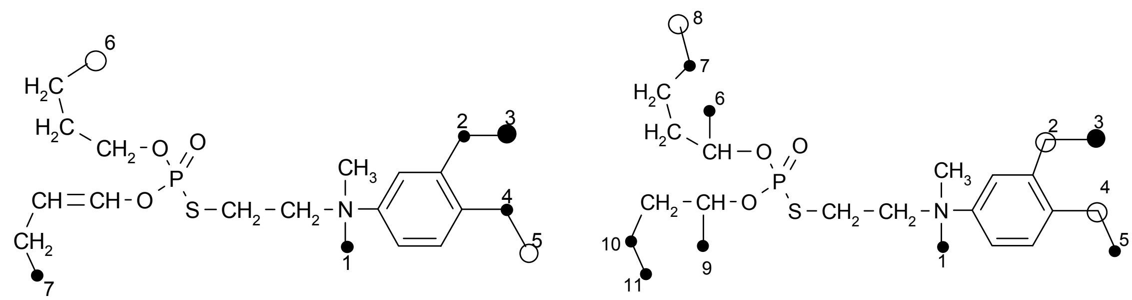

(24)

Fig. 5 – Hypermolecule and optimized receptor maps for acetylcholinesterase phosphorylation by phosphororganic derivatives, series (24) and (25).

Several QSAR's were established for a series of N = 97 phenyl substituted methyl phenylcarbamates.[78,79] With Hansch hydrophobicities, σ-Hammett constants, molar refraction and charge transfer character for the substituent R, $r^2 = 0.58$ is obtained. Addition of MSD with respect to R of the most active molecule, gives, $r^2 = 0.64$. A study with the MTD – method[79] yields , $r^2 = 0.76$ with MTD for the best optimized receptor map, depicted in Fig. 6 and the structural parameters of the previous paper. Five different start maps resulted in five different optimized map; the optimized map of Fig. 6 does not respect the single – connected condition for cavity plus common core vertices (see chap. 3).

The QSAR's for these two classes of AchE inhibitors have, as common characteristics, the dependence on the reactivity of the leaving group (σ-Hammett types constant) and are often favoured by a positive charge in this group. The rather variable QSAR results suggest different inhibitory mechanism, possibly by different spatial orientations of molecules adsorbed on AChE in the neighborhood of the catalytic site.

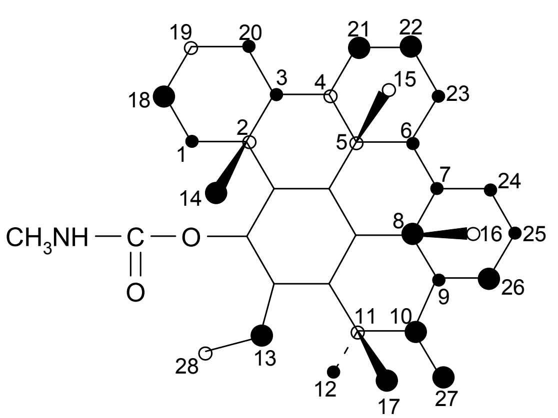

Fig. 6 – Optimized receptor map for AChE inhibition by phenyl-methyl-carbamates.[79] Cavity vertices j:16, 19 and 28 are isolated from the rest of cavity plus common core vertices which form a single connected graph. Significance of o, ●, • vertices, see Fig. 3.

SOLUBILITY AND STERIC PARAMETERS

Crystallization takes place usually with a single type of molecule. Cocrystallization is also often favored by similar shapes (of the main type and inclusion ions). In order to test if solubilities depend also on the shape similarity between solvent and solute molecules we correlated series of organic solvent: water partition coefficients ($\log P_{solv:aq}$) with the MSD value of solute molecules with respect to the solvent molecule.[80,81] For nitrobenzene as organic solvent, for logP *vs.* MSD correlation, for N = 16 organic molecules r = - 0.093 is obtained for toulene as organic solvent, N = 63; r = -0.177; for isobutanole, N = 103; r = 0.138; for 2-butanone, N = 7; r = -0.518. Experimental $\log P_{solv}$ data are from Leo, Hansch and Elkins.[82]

Thus molecular shape, molecular similarity with the solvent molecule, are not correlated to solubility.

REGULATION OF PROTEIN KINASES BY C-AMP DERIVATIVES

The secondary messenger, cAMP binds against two classes of binding sites, A and B, of two types of protein kinases, cAKI and II, which are implied in regulation of cell proliferation. Finding cAMP derivatives binding more selective to these sites could be interesting for chemotherapy of cancer and other diseases.[83]

QSAR-MTD studies were performed for each of the four binding sites (AI, AII, BI, BII) separately with affinities to these sites as biologic activities. First, a series of N = 27 cAMP derivatives with relatively small substituents in purine-position 1, 2, 6 and 8 (and N vs. substitution within the purine moiety), together with some (equatorial and axial) thiophosphoric acid derivatives were considered; the hypermolecule (Fig. 7) has M = 14 vertices.[84] Other structural variables – $\log K_W$ – nitrogen base hydrophobicity; q_6 – electric charge in purinic position 6; indicator variable $\delta = 1$ for equatorial S atom ($\delta = 0$ otherwise). For binding to the AI site (A of cAKI) the optimized receptor map is depicted in Fig. 7, the correlational equation and results are:

$$\hat{Y} = 1.171 - 2.004\delta + 1.836q_6 - 0.452\text{MTD};\ r^2 = 0.90;\ r_{CV}^2 = 0.85 \qquad (27)$$

For all four binding sites, the correlational results are in the range $r^2 = 0.70 - 0.93$, $r_{CV}^2 = 0.40 - 0.85$, not always satisfactory.[84]

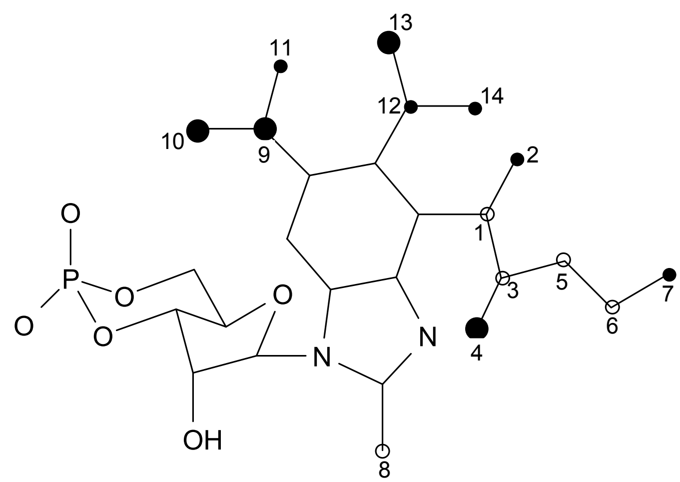

Fig. 7 – Vertex j numbering and optimized receptor map for cAMP derivatives – affinity towards the A-side of the cAKI-kinase[83]. Significance of o, ●, • vertices, see Fig. 3.

The same method and correlational (EVEN/ODD) procedure was applied to a series of N = 94 cAMP derivatives with large substituents in positions 2, 6 and 8 (M = 74 vertices) with correlational results in the $r^2 = 0.53 - 0.96$, $r_{CV}^2 = 0.36 - 0.64$ range.[85] Two separate studies were performed for molecules with large substituents in position 2 (N = 21, M = 14) and with large, partially quiral substituents in position 8 (N = 32, M = 21), with the same type of structural parameters.[85]

The combination of the four hypermolecules span a total of M = 67 vertices, 6 of which are common to 3 hypermolecules, other 33 to 2 hypermolecules. Comparing the attribution of common vertices, only five have different attribution in the 3 papers.[84-86] Of the results, for the AI and BI receptors a high q_6 –positive charge is beneficial for binding. BI and BII sites have a marked hydrophobic character. Thiophosphoric (equatorial S atom) derivatives have a decreased affinity for all four receptors.[83] Protonated (at pH 6) aliphatic chain ω-NH_2 groups (2 and 8 substituents) reduce affinity.[85] Differences between the receptor maps for the four sites could be used to attempt synthesis of cAMP derivatives with specific binding against one of these sites.

CARCINOGENESIS AND ANTICANCER AGENTS

For polycyclic aromatic hydrocarbon derivatives with mutagenic/carcinogenic activity based upon diol derivatives, cation stabilization energy is a usefull parameter. For a series of derivatives of benzopiren, benzantracene, colantrene and methylated derivatives we tried to correlate carcinogenicity with the cation delocalization energy, DE (ω-HMO method), MTD and average topologic distance connectivity, j. For the very active compounds, Y = 1.5 was considered as the quotient of animals with tumors per total number of animals for moderately active compounds and Y = -0.5 for inactive compounds. The correlation with DE is already significant and is markedly increased by adding MTD as a second parameter, but only moderately by adding j as the third. Out of a total N = 53 PAH – derivatives, 41 were correctly classified into the 3 activity classes and there were no false prediction between the 2 extreme classes (very active and inactive).[87]

QSAR's with MSD and MTD were attempted for *cis* dichlorodiamine platinum(II) compounds with various ammine ligands, which act by cross-alkylating nitrogen bases within DNA.[88] Toxicity in mice and therapeutic index against the ADJ/PC6 tumor were used as biologic activities. A decrease of toxicity with increase of hydrophobicity π was observed (N= 17, $r^2 = 0.79$), but, for the therapeutic index there is no such correlation ($r^2 = 0.16$). Addition of MSD or MTD to the correlation with the therapeutic index produces an $r^2 \approx 0.50$. In a more recent study,[89] for N = 24 complexes with aliphatic monoamines, toxicity correlates well with π and π^2 ($r^2 = 0.79$) and an optimal hydrophobicity of $\pi = 2.5$ is indicated. Addition of MTD yields $r^2 \approx 0.75$ and the detrimental vertices of the receptor map indicate steric hindrance effects in the attack upon DNA. For a more complete series of N = 45 complexes including bidentate ligands and a more complete series of N = 45 complexes including bidentate ligands and a more complete series of leaving groups (Cl^-, Br^-, I^-, $C_2O_4^{2-}$, etc.) an attempt to factorise toxicity and therapeutic index on amine and leaving group failed, but the dependence of toxicity upon π is, at least qualitatively, the same.[89] A theoretical study, at the EHT-level for this type of complexes was also performed.[90] Correlation of antitumor activity with MSD was also attempted for a series of Cu(II)-aminoacid complexes.[91]

QSAR's by MTD were performed also for reversal of keratinisation of hamster tracheal organ culture, for a series of N = 53 retinoids including *all trans* and *13-cis* retinoic acid esters, amides, various ring and side chain modified analogs.[92] A hypermolecule with M = 63 vertices results. The optimized receptor map was obtained with the single connex graph restraint for cavity and common core vertices. The correlational result is $r^2 = 0.73$, while for a test series of N = 15 other retinoids, $r^2_{CV} = 0.84$ is obtained. A revised version of this MTD, for a more extended series of retinoids was also published.[93]

BIOLOGICALY ACTIVE STEROIDS

A series of N = 46 cardenolipides and bufadienolides-toxicity with respect to cats as biological activity, yields good correlation with MTD (single connected graph condition for cavity and common vertices respected) – $r^2 = 0.72$ is obtained.[27] Inclusion of hydrophobicity produces only a moderate increase, to $r^2 = 0.84$. For crossvalidational tests, see previous chap. 3. In another series of N = 20 digitoxigenin, digoxigenin derivatives with small substituents, the correlational result is:[94]

$$\hat{Y} = 7.383 - 0.753\mathrm{MTD} - 0.923\delta_7 ; \qquad r^2 = 0.84 \tag{28}$$

with δ_7 for strong inhibitory effects of C15-substituents. Inhibition of Na^+/K^+-ATPase was considered in[94]. Order of experimental activities for some common compounds differ in[94] and[27], as well as the optimized receptor maps.

For gestagenic steroids, good results where obtained with MTD asd hydrophobicity, π. For a series of N = 34 progesterone derivatives $r^2 = 0.93$ is obtained ($r^2 = 0.49$ with π only)[25], for a series of N = 25 testosterone derivatives $r^2 = 0.92$ is obtained.[86] In a MTD-QSAR for a series of N = 55 progesterone, 4,9 estradien-3-one and 5αH-androstane-3one derivatives, with MTD and π, $r^2 = 0.87$ is obtained;[27] for a test series of 5 different steroids, the calculated vs experimental activity correlation yields $r_{CV}^2 = 0.50$.

QSAR's were established also for estrogenic steroids. For a series of N = 22 estradiol and stilbestrol derivatives, $r^2 = 0.95$ was obtained[98], but for a very large number (M = 50) of vertices, with MTD and π. For a series N = 30 estrogenic derivatives, with Se and I atoms in substituents, $r^2 = 0.85$ was obtained, with MTD and two indicators variables (for the presence of the key 3 and 17β oxygen atoms).[99]

For a series of N = 46 aromatase inhibiting steroids, $r^2 = 0.83$ was obtained with MTD, π and the resonance energy, R, for a system of conjugated electrons in the region of the A and B rings.[100]

QSAR's with MTD were performed also a series of N = 21 steroids, *vs.* affinity to Corticosteroid Binding Protein and Testosterone Binding Proteins.[101] The results were $r^2 = 0.93$ and $r^2 = 0.85$, but for a test series of 10 different steroids, the CoMFA-QSAR[102] gives better prediction than this MTD-QSAR.

MTD WITH ORTHOGONALIZATION OF PARTNER DESCRIPTORS

Within the MTD-method, variation of the MTD descriptor values and other, partner, descriptor value can be performed with orthogonalization of the descriptors such that MTD retains mainly information not contained in the partner descriptors. This method was applied to a series of N = 49 psychotomimetic phenylalkylamine derivatives.[103] As partner electronic descriptors, the energy of the lowest unoccupied orbital was used, together with the net charges on the phenyl ring atoms (AM1 calculations). Other descriptors used within various models were hydrophobicity and lipophilicity descriptors and Hall and Kier electrotopological state descriptors. The descriptors used were scaled to unit and orthogonalized by a method of Randić. The resulted hypermolecule has M = 20 vertices. As statistical results $r^2 = 0.885$ and $q^2 = 0.793$ were obtained. The Randić orthogonalization identifies MTD as a dominat descriptor which was separated from the information related to other descriptors.[103]

The MTD method was used also in connection with hydrophobicity upon a series of N = 20 polychlorinated biphenyl derivatives and N = 12 polychlorinated benzene derivatives, for which reliable experimental data are available.[104] When MTD is used in association with descriptors related to topological 2D and 3D properties, most tested descriptors correlate strongly with the number of chlorine atoms. For the polychlorinated biphenyl derivatives (M = 10 vertices) logarithms of water: octanole partition coefficients yield, in correlation with the number of chlorine atoms yields $r^2 = 0.931$, while correlation with MTD yields $r^2 = 0.948$ – with supplementary information for proximity effects,

Several other QSAR's with MTD were also performed for series of amphetamine type derivatives and other small aromatic molecules with biologic activity as well as conformational analysis and calculations of thermodynamic properties, by quantum chemistry methods, for representative molecules.[105-107]

QUANTITATIVE STRUCTURE-ACTIVITY/PROPERTY RELATIONSHIPS APPLIED TO DYE LIPOPHILICITY, BIODEGRADABILITY AND AFFINITY FOR FIBRE, POLYMER TECHNICAL PROPERTIES AND CHROMATOGRAPHIC MOBILITIES

Dyeing can be seen as an apparently simple process which is actually rather difficult to explain. There appears to be a decrease in entropy (an increase in the order of the dye molecules). The explanation for this lies probably in the complexity of the whole system (including the complex structure of water itself). However, the fact that such phase transfers involving the adsorption of large ions or molecules from one phase to another occur is rather fortunate in other fields.

Molecular modeling and statistical methods used in the QSAR (Quantitative Structure-Activity Relationships) field constitute important new tools for the study of dye-fibre interactions. The advantages of this new approach to dye adsorption on cellulose fibre are related either to the description of the mechanisms present at the molecular level or to the predictability of the proposed models, which can lead to the design of new dyes with higher affinities for the cellulose fibre.

Classical QSAR, pattern recognition and 3D-QSAR methods have been employed by us in the study of dye fibre interactions.[66, 67, 111-130] Several classes of dyes were used in the study of the application of QSAR techniques to cellulose dyeing. Multiple linear regression (MLR) and principal component regression (PCRA) methods applied to a series of anthraquinone vat dyes lead to the conclusion that among the most important parameters in this dye series are the length of the conjugated chain of the dye molecule and the number of proton donor groups.[114-116] Minimum steric difference (MTD) results obtained for planar[114,115,118] and multiconformational[117] constructions showed a similar conclusion, that along the longest dye molecule axis mainly attractive interactions are present; only in lateral pockets were some detrimental vertices found. The comparative molecular field analysis (CoMFA) study leads to the conclusion that the electrostatic interaction is the main factor contributing to the dye-fibre interactions.[117] The electrostatic field contributions show that, if vast domains exhibit increasing positive charges, *i.e.*, in the regions of almost all substituents of the anthraquinone moiety, this should yield higher affinities for cellulose. This fact suggests some kind of electrostatic “attraction” between the dye molecule and the negatively charged cellulose fibre. This is in accordance with the results of the MTD method, showing attractive regions for many vertices of the substituents belonging to the anthraquinone skeleton. It is interesting however that the analysis of the CoMFA steric field contributions leads to the conclusion that the beta substitution to the anthracene moiety will reduce dye affinity, in contradiction to the MTD results, which indicate this region as beneficial for binding.

Series of anionic monoazo dyes were studied by 2D-QSAR methods.[119] Dye lipophilicity, expressed by the chromatographic R_M values, has been found to have contribution to dye affinity for compounds with one, respectively two sulphonic acid groups in the coupling component, as derived from MLR models. Electronic effects (expressed by frontier orbital energies) are also important in dye adsorption. MTD results[119] indicated as favorable region of dye binding the molecular dye axis and the inclusion of additional condensed aromatic nuclei. The presence of sulphonic acid groups in the dye molecule was detrimental for dye adsorption on cellulose, which contributed only to dye solubilization. Steric effects were found to be important in dye-cellulose interactions for this series of compounds. CoMFA results were obtained for electronic dye structures characterized by gas/solution-phase chemical descriptors.[120,121] In both cases local positive charges and increased dye donor ability favored the dye adsorption on negatively charged cellulose. In the first case predominance of electrostatic interactions in cellulose dyeing was observed, and hydrogen bonds as crucial feature in the dye-fibre interactions, which may also be involved in intermolecular dye-dye aggregation, in the second case. Specific binding affinity in terms of pharmacophoric constraints, even less specific than ligand-biological receptor interactions, was also discussed.

A MTD study was performed for a series of heterocyclic monoazo dyes.[122] Dye binding was observed in regions along the dye molecular axis. Additional condensed aromatic nuclei in the heterocyclic dye moiety favored the dye affinity for cellulose, in opposition to sulphonic groups contained in the dye molecules.

MTD calculations were applied to another series of heterocyclic azo dyes[123] and dye binding to cellulose fibre was observed in regions along the dye molecular axis. Sulphonic groups attached to the dye molecules caused steric repulsions with the fibre. A deeper insight in dye-cellulose interactions was obtained by CoMFA.[124] The CoMFA results indicated that electrostatic field contributions, dominant, bulky groups attached to the naphthyl moiety and predominance of positive over the negative charges to be important for dye adsorption. The contribution of dye molecule solvation in cellulose dyeing was considered by the contribution of the LUMO molecular orbital energy.

For a series of bisazo anionic dyes MLR and NN studies were performed using a set of steric, electronic and hydrophobic parameters derived from three-dimensional dye structures.[67] Important steric and electrostatic effects were found in dye binding, also dye adsorption to be favored along the longest dye molecular axis and by the shape of dye molecules. The dye donor ability of dye molecules in dye-fibre interactions was found to be important for dye-cellulose binding too. The NN calculations emphasized strong nonlinear dependence of dye descriptors with their affinity for cellulose. CoMFA results[125] emphasized the dominant electrostatic field contribution in dye-fibre interactions and the molecular dye planarity and inclusion of the J-acid in the coupling component as favorable for dye affinity.

The affinity for cellulose fibre of a series of disperse dyes was first studied by means of the Free-Wilson and the MLR methods.[126] Electronic effects were found to be significant in dye binding to fibre. Dominant steric effects for dye affinity could be explained by the importance of dye linearity and coplanarity which favor dye adsorption, as well as the increasing dye molecular length. MTD results indicated the beneficial region of binding along the longest molecular axis and addition of heterocyclic condensed substituents favorable for dye binding. CoMFA analysis applied to the same series of dyes[127] yielded the conclusion of steric field contributions dominant over the electrostatic ones for dye adsorption and increased heterocyclic area in dye molecules favorable for dye affinity. This was in contradiction to the results obtained for anthraquinone vat dyes and for monoazo and bisazo dyes. Positive electrostatic contribution around the benzene ring bonded to the azo group are favorable for dye binding. The pharmacophoric concept hypothesis which states that micro-crystalline states from the cellulose fibres create a binding site similar to the enzymatic binding site, which recognizes molecular patterns of dye molecules was questioned for this series of dyes.

Taking into account the above presented QSAR-type results applied to dye adsorption on cellulose, an appreciable similarity of dye-fibre interactions with receptor-ligand interactions was concluded. Structural dye features favorable for binding to cellulose obtained by QSAR-type calculations were reviewed in a few articles.[66,128-130]

Quantitative Structure-Property Relationships (QSPR) have been applied to study technical polymer properties by our group. Principal component analysis (PCA), molecular modeling and multiple linear regression (MLR) were applied to model the glass transition temperature of some polyphosphonates (phosphates) which are important because of their excellent mechanical, electrical and flame resistance properties and also because of their analogy with the nucleic acids.[131-133] A step-by-step build-up approach (*e.g.*, generation of structures by joining together smaller fragments in known low energy structures) and molecular modeling calculations were used to study the possible conformations of $PhOP(O)(Me)OPh(Me)_2Ph$.[132] The conformations of low, comparable energy levels were employed to construct the most stable dimer and tetramer of the polymer. Starting from structures of low energy monomer conformations structural parameters of several polyphosphates and polyphosphonates were calculated and further used in correlations with the polymer glass transition temperatures.[133] Structural polymer features important for the glass transition temperature were analyzed qualitatively (by principal component analysis) and quantitatively (by multiple linear regression). Structural polymer features important for the glass transition temperature were emphasized.

Kaliszan[134] considers that same kind of basic intermolecular interactions determine the behaviour of chemical compounds both in biological and chromatographic fields. Quantitative Structure-Retention Relationships (QSRR) were applied by us to chromatographic mobilities of several series of compounds.[135-142] Thus, enantioselectivity of oxirane ring-opening catalyzed by epoxide hydrolases was studied by multiple linear regression and by artificial neural networks (ANN).[135] Steric and/or electronic requirements for the enantioselectivity in substrate binding were found from the influence of structural parameters of epoxides on enantioselectivity.

Quantitative structure-retention (QSRR), as well as enantioselective retention relationships (QSERR) were derived by multiple linear regression analysis, artificial neuronal network and CoMFA calculations for a series of chiral arylalkylcarbinols on four brush-type chiral stationary phases.[136,137] Electronic structural properties and – less important – the distance from the chiral carbon atom to the last non-hydrogen atom of the alkylcarbinol moiety were found to be important for the chromatographic capacity factors. For the enantioselectivity in QSERR models bulk (or steric) as well as polar or electrostatic properties of analytes were important. This finding was in line with the CoMFA results where steric and electrostatic fields were found to contribute almost equally with a slight dominance of the electrostatic interactions.

QSRR calculations were also applied to model the chromatographic mobilities of some 4,4'-diaminobenzanilide-based direct dyes.[138-140] Traditional and rational QSAR/QSPR modelling techniques have been applied to find a quantitative structure-retention relationship: molecular modelling, multiple linear regression and principal component analysis. Influence of structural dye parameters indicated the importance of dye hydrophobicity, dye molecular dimension and structural complexity on their lipophilicity.

Chromatographic mobilities of a series of arylamides of ortho-hydroxyarylcarboxylic acid was studied by QSRR.[141,142] Molecular modeling, principal component analysis (PCA), principal component regression analysis (PCRA) and multiple linear regression (MLR) were applied to study the influence of structural descriptors on the chromatographic mobilities. It was found that arylamide lipophilicity depended on polarity and bulk terms.

A hydrophobicity, protolytic equilibrium and chromatographic behaviour study of some monoazoic dyes[143] was performed by statistical analysis. The neutral, amphionic and ionic dye forms were studied in assessing chromatographic mobilities for lipophilicity characterizations and the importance in partition processes of ionic and amphionic dye forms. Correlations between experimental chromatographic mobilities and calculated octanol-water partition coefficients indicated that not only neutral but also amphionic, possibly also ionic forms brought a substantial contribution to polar–lipophilic partition processes.

QSAR methods are also employed for the prediction of acute toxicity of chemical compounds when experimental data are few or do not exist. Textile dyes have to be removed before slooping in rivers because they are easily recognized in wastewaters. Such compounds can reach the aquatic environment as dissolved or suspended dyestuff because the usual conventional treatments employed in the textile and synthesis dye factories do not remove efficiently most dyes. Aerobic biodegradability of some sulphonated azo dyes was studied by principal component analysis and the discriminant technique of two-value regression analysis.[144] The derived results emphasized the interaction between ring substituents for dye biodegradability. A statistically significant and biologically meaningful regression model that gives perfect classification was obtained, and the results were compared with the previous qualitative interpretation of the substituent effects on biodegradation.

CONCLUSIONS

The main interest in the QSAR-group of Timişoara was the inclusion of molecular stereochemistry in QSAR. The MSD and the MTD methods are the most often quoted results of this group but other items, such as molecular shape descriptors based upon the molecular van der Waals space and new topologic indices also contributed to inclusion of stereochemistry in QSAR.

The MTD method is a recognized as a precursor of modern 3D-QSAR. Most QSAR-books written in the eighties quote MTD. The molecular superposition procedure, successfully used by MTD, is used also by CoMFA – the finally adopted as standard – method. Instead of the hypermolecule of MTD, based on the superposed molecules, CoMFA uses another network, the vertices of which could correspond to the approximate position of receptor atoms. The MTD-method was among the first QSAR-methods to use, on a large scale, test series of molecular in order to have a, at least somewhat realistic, idea on the predictive power of results. The inability of our group to create a user's friendly program for hypermolecule construction limited the use of MTD by other groups.

Several QSAR applications of MTD and molecular shape descriptors were realized by the QSAR group of Timişoara and in collaboration with other groups interested in QSAR. The most quoted applicational line is the one related to the affinity of dyes to cellulose fibers – considering the textile fiber analogous to biologic receptors; not only MTD but also several modern methods, such as CoMFA or neural networks were used hereby. In last years, studies based on modern drug design techniques, concerning receptor-ligand interactions and studies based on search techniques in large data bases, have also been developed.

REFERENCES

1. C. Hansch and T. Fujita, *J. Amer. Chem. Soc.,* **1964**, *86*, 1616.
2. R. Valceanu, Z. Szabadai, A. Chiriac and Z. Simon, *Studia Biophys* (Berlin), **1972**, *34*, 1.
3. Z. Szabadai and Z. Simon, *Rev. Roum. Chim.,* **1972**, *9*, 327.
4. I. Simiti and J. Schwartz, "Structura chimică. Activitate biologică" (Chemical Structure. Biological Activity), Ed. Dacia, Cluj, 1974.
5. Z. Simon and Z. Szabadai, *Studia Biophys* (Berlin), **1973**, *39*, 123.
6. E. Fischer, *Chem. Ber.,* **1894**, *27*, 2985.
7. E. J. Amoore, G. Palmieri and E. Wanke, *Nature,* **1967**, *216*, 1084.
8. N. L. Allinger, "Pharmacology and the Future of Man. Proceedings of the 5th International Congress of Pharmacology", R. A. Maxwell, editor Karges, Basel, 1972, p. 7.
9. A. T. Balaban, A. Chiriac, I. Motoc and Z. Simon, "Steric Fit in QSAR", Springer. Berlin (Lecture Notes in Chemistry Series), 1980.
10. Z. Simon, A. Chiriac, S. Holban, D. Ciubotariu, G. I. Mihalas, "Minimum Steric Difference. The MTD Method for QSAR Studies", Res. Studies Press (Wiley), Letchworth, 1984.
11. J. Järv, T. Kesvatera and A. Aaviksaar, *Eur. J. Biochem*, **1976**, *67*, 315.
12. D. Ciubotariu, E. Deretey, T. I. Oprea, T. Sulea, Z. Simon, L. Kurunczi and A. Chiriac, *Quant. Struct. Act. Relat.,* **1993**, *12*, 367.
13. Analysis of Ligand-Protein Contact in PDB-entry 2ACE: http://pdb_browsers.ebi.ac.uk/pdb_docs/L1G1M/AC/1ACL_lig01/1ACL_lig01.html
14. Z. Simon, A. Chiriac, I. Motoc, S. Holban, D. Ciubotariu and Z. Szabadai, *Studia Biophys* (Berlin), **1976**, *55*, 217.
15. Z. Simon, "Drug Design. Theory. Methods. Applications", H. Kubinyi, editor, ESCOM, Leyden, 1993, p. 307.

16. I. Motoc, *Math. Chem*., **1978**, *4*, 113.
17. I. I. Badilescu and Z. Simon, *Rev. Roum. Biochimie* **1976**, *13*, 239.
18. Z. Simon, I. I. Badilescu and T. Racovitan, *J. Theoret. Biol.*, **1977**, *66*, 485.
19. C. Silipo and C. Hansch, *J. Amer. Chem. Soc*., **1975**, *97,* 6849.
20. A. Chiriac, Veronica Chiriac, D. Ciubotariu, S. Holban and Z. Simon, *Eur. J. Medic. Chem.*, **1983**, *18*, 507.
21. T. Sulea, L. Kurunczi, T. I. Oprea and Z. Simon, *J. Comput. Aided Molec. Des.***,1998**, *12*, 133
22. I. Motoc and I. Dragomir-Filimonescu*, Math. Chem.,* **1981**, *12*, 117.
23. I. Motoc and I. Dragomir-Filimonescu, *Math. Chem.,* **1981**, *12*, 127.
24. I. Motoc, *Arzneim. Forsch.* **1981**, *91*, 290.
25. V. Austel, E. Kulter and W. Kalbfleisch, *Arzneim. Forsch.*, **1979**, *23*, 585.
26. R. F. Rekker, "The Hydrophobic Fragmental Constant", Elsevier. Amsterdam, 1977, Appendix.
27. Z. Simon, M. Dragomir, M. G. Plauchithiu, S. Holban, H. Glatt and F. Kerek, *Eur. J. Med. Chem.,* **1980**, *15*, 521.
28. Z. Simon, *Math. Chem.*, **1982**, *13*, 356.
29. I. Motoc, "Steric Effects in Drug Design", M. Charton and I. Motoc, eds (Topics in Current Chemistry Series), Springer, Berlin, 1983, p. 94 – 105.
30. R. Cramer, III, D. Patterson and J. Bunce, *J. Amer. Chem. Soc.,* **1988**, *11*0, 5959.
31. J. G. Topliss and R. J. Costello, *J. Medic. Chem.,* **1972**, *15*, 1066.
32. J. G. Topliss and P. P. Edwards, *J. Medic. Chem.,* **1979**, *22*, 1238.
33. Z. Simon, *Rev. Roum. Chim.,* **1987**, *32*, 1103.
34. T. I. Oprea, L. Kurunczi, M. Olah and Z. Simon, *SAR and QSAR in Envir. Res.,* **2001**, *12*, 75.
35. Z. Simon, S. Muresan, T. Sulea, A. Chiriac and D. Ciubotariu, *Rev. Roum. Chim.*, **1997**, *42*, 1083.
36. T. I. Oprea and G. R. Marshall, *Perspect. Drug Discovery Des.,* **1998,** *9-11*, 35.
37. V. A. Palyulin, E. V. Radchenko and N. S. Zephirov, *J. Chem. Inf. Comput. Sci.,* **2000,** *40*, 695.
38. T. Sulea, L. Kurunczi and Z. Simon, *SAR and QSAR in Envir. Res.,* **1995**, *3*, 37.
39. L. Kurunczi, M. Olah, T. I. Oprea, C. Bologa and Z. Simon, *J. Chem. Inf. Comput. Sci.,* **2002**, *42*, 841.
40. HyperChem 5.11 Pro and ChemPlus 1.6 – Hyper Cube Inc. packages http://www.hyper.com
41. L. Kurunczi, E. Seclaman, T. I. Oprea, L. Crisan and Z. Simon, *J. Chem. Inf. Model.,* **2005**, *45*, 1275.
42. D. Ciubotariu, V. Gogonea and M. Medeleanu, "QSAR Studies by Molecular Descriptors", M. V. Diudea editor, Nova Science Publ. Inc., Huntington New York, 2001, chap. 10, p. 281.
43. D. Ciubotariu, S. Holban and I. Motoc, *Preprint Univ Timis, Fac. Stiinte ale Naturii,* Sectia Chimie, **1975**, *3*, 1.
44. I. Motoc, N. Dragomir-Filimonescu and R. Valceanu, *Math. Chem.,* **1981**, *11*, 185.
45. V. Gogonea, D. Ciubotariu, E. Derety, M. Popescu, I. Iorga and M. Medeleanu, *Rev. Roum. Chim*., **1991**, *36*, 465.
46. I. Motoc, D. Ciubotariu, S. Holban, *J. Polym. Sci*., **197**7, *15*, 467.
47. I. Motoc, S. Holban and R. Vancea, in[9], chap. 6, p. 108.
48. D. Ciubotariu, E. Deretey, M. Medeleanu, V. Gogonea, S. Muresan, A. Novac, C. Bologa and Z. Simon, "Trends in QSAR and Molecular Modelling. 9th Proc. Eur. Symp. Struct. Act. Relat. Mol. Modell.", CG Wermuth, editor, ESCOM, Leyden, 1993, p. 385.
49. M. Medeleanu, D. Dragos, T. Olariu, V. Vlaia, C. Ciubotariu, Corina Seiman and D. Ciubotariu, *Bull. Politehnica Univ.,* **2004**, *49*, 8.
50. D. Ciubotariu, Doctoral Thesis, Inst. Polit. Bucureşti, **1987**.
51. D. Dragos, Doctoral Thesis, West Univ. Timişoara, **2005**.
52. R. Vancea, S. Holban and D. Ciubotariu, "Recunoaşterea formelor. Aplicaţii (Pattern Recognition. Applications)", Ed. Academiei, Bucureşti, 1989.
53. D. Dragos, A. Heghes, M. Medeleanu, V. Vlaia, Corina Seiman, A. Kaycsa, D. Ciubotariu, *Timisoara Med. J.*, **2004**, *54*, 128.
54. D. Ciubotariu, S. Muresan, V. Gogonea, C. Baleanu-Gogonea, M. Medeleanu. C. Ciubotariu, M. Popescu, *Roum. Biotechnol. Lett.,* **1997**, *2*, 114.
55. I. Motoc, *Math. Chem.,* **1979**, *5*, 275.
56. P. H. Sellers, Siam, *J. Appl. Math.,* **1974**, *2*6, 787.
57. D. Ciubotariu, M. Medeleanu and V. Gogonea, *Chem. Bull. Tech. Univ.,* **1995**, *40*, 21.
58. D. Ciubotariu, M. Medeleanu, V. Vlaia, T. Olariu, C. Ciubotariu, D. Dragos, Corina Seiman, Molecules, **2004**, *49*, 14.
59. A. T. Balaban, D. Ciubotariu and O. Ivanciuc*, Math. Chem.,***1990**, *25*, 41.
60. M. Medeleanu and A. T. Balaban, *J. Chem. Inf. Comput. Sci.,* **1998**, *38*, 1038.
61. D. Ciubotariu, M. Medeleanu and V. Gogonea, *Chem. Bull Univ. Tms.,* **1996**, *41*, 19.
62. D. Ciubotariu, M. Medeleanu and V. Gogonea, *Chem. Bull Univ. Tms.,* **1995**, *40*, 21.
63. A. T. Balaban, d. Ciubotariu and M. Medeleanu, *J. Chem. Inf. Comput. Sci.,* **1991**, *31*, 517.
64. Speranta Avram, C. Bologa, Magdalena Banda and Maria Luiza Flonta, *Roumanian J. Biophys.,* **2001**, *11*, 11.
65. Speranta Avram, I. Svab, C. Bologa, and Maria Luiza Flonta, *J. Cell. Molec. Mod.*, **2003**, *7*, 286.
66. Simona Timofei, L. Kurunczi, W. Schmidt and Z. Simon, *SAR and QSAR in Envir. Res.,* **2002**, *13*, 219.
67. Simona Timofei, L. Kurunczi, T. Suzuki, W. M. Fabian and S. Muresan, *Dyes Pigm.*, **1997**, *34*, 183.
68. S. Muresan, T. Sulea, D. Ciubotariu, L. Kurunczi, and Z. Simon, *Quant. Struct. Act. Relat.,* **1996**, *15*, 31.
69. T. Sulea, T. I. Oprea, S. Muresan and S. I. Chan, *J. Chem. Inf. Comput. Sci.,* **1997**, *37*, 1162.
70. Liliana Ostopovici, T. I. Oprea, Maria Mracec, C. Bologa, M. Mracec, "Cheminformatics in Drug Discovery", T. I. Oprea editor, Wiley-VCH-Verlag GmbH&Co, KGa A, vol. 32, 2004, p. 223–239.
71. M. I. Kabachnik, A. P. Brestkin and M. Y. Michelson, "Mechanism of Action of Phosphororganic Compounds" (in Russian), IXth Mendeleev Session, Nauka Publ. House, Moscow, 1965, p. 161.
72. R. D. O'Brien, "Chimie organique du phosphore. Colloques internationales CNRS", Editions CNRS, Paris, 1969, p. 353.
73. R. Valceanu, A. Chiriac and Z. Simon, *Rev. Roum. Biochimie,* **1973**, *10*, 239.

74. A. Chiriac and Veronica Chiriac, *Analele Univ. Tms. Ser. Fiz. Chim.,* **1976**, *XIV*, 45.
75. A. Chiriac, Veronica Chiriac and Z. Simon, *Preprint Univ. Timisoara, Ser. Chim.,* **1979**, 2.
76. A. Chiriac, D. Ciubotariu, Z. Szabadai, R. Valceanu and Z. Simon, *Stud. Biophys* (Berlin), **1975**, *51*, 183.
77. R. Valceanu, A. Chiriac, Z. Szabadai and Z. Simon, *Analele Univ. Tms. Ser. Fiz. Chim.,* **1977**, *XV*, 61.
78. A. Chiriac, D. Ciubotariu, Z. Szabadai, R. Valceanu and Z. Simon, *Rev. Roum. Biochimie,* **1975**, *12*, 143.
79. I. I. Badilescu, A Stepan, A. Chiriac and Z. Simon, *Analele Univ. Tms. Ser. Fiz. Chim.*, **1978**, *XIV*, 29.
80. Elisabeta Schuch-Draskovits, S. Holban, D. Ciubotariu and Z. Simon, *Analele Univ. Tms. Ser. Fiz. Chim.*, **1979**, *XVII*, 73.
81. Z. Simon and Elisabeta Draskovits, *Rev. Roum. Chim.*, **1977**, *22*, 87.
82. A. Leo, C. Hansch and D. Elkins, *Chem. Revs.*, **1971**, *71*, 525.
83. N. Nass, C. Colling. M. Cramer, G. H. Genieser, E. Butt, E. Winkler, L. Janicke and B. Jastorff, *Biochem. J.*, **1992**, *285*, 129.
84. S. Muresan, C. Bologa, A. Chiriac, B. Jastorff, L. Kurunczi and Z. Simon, *Quant. Struct. Act. Relat.*, **1994**, *13*, 242.
85. S. Muresan, C. Bologa, M. Mracec, A. Chiriac, B. Jastorff, Z. Simon and G. Naray-Szabo, *J. Mol. Struct (Theochem)*, **1995**, *142*, 161.
86. Susanne Liauw, F. Iwitzki, S. Muresan, C. Bologa, A. Chiriac, L. Kurunczi, Z. Simon and B. Jastorff, *Rev. Roum. Chim.*, **1998**, *43*, 241.
87. Z. Simon, A. T. Balaban, D. Ciubotariu and T. S. Balaban, Rev. Roum. Chimie, **1985**, *30*, 985.
88. Z. Simon, Maria Mracec, Ana Maurer, Septimia Policec and C. Dragulescu, *Rev. Roum. Chim.*, **1977**, *14*, 117.
89. Maria Mracec, M. Mracec and Z. Simon, *Rev. Roum. Chim.*, **1997**, *42*, 799.
90. Maria Mracec, M. Maurer, Septimia Policec, Ana Maurer and Otilia Costisor, *Ann. West. Univ. Timişoara, Ser. Chim.*, **1995**, *1*, 75.
91. C. Dragulescu, Maria Mracec, Z. Simon, Septimia Policec, V. Topciu and N Csaki, *Bul. Stiintif. Tech. Inst. Polit Traian Vuia*, **1979**, *24*, 71.
92. I. Niculescu-Duvaz, Z. Simon and N. Voiculetz, "Chemistry and Biology of Synthetic Steroids", Marcia Dawson and W. Okamura, eds, CRC-Press, Boca Raton, Flo, 1990, p. 579.
93. D. Ciubotariu, A. Grozav, V. Gogonea, C. Ciubotariu, D. Dragos, M. Pasare and Z. Simon, *Math. Computer Chem.*, **2000**, *41*, 107.
94. A. Bohl and Z. Simon, *Z. Naturforsch.*, **1984**, *40c*, 858.
95. M. Bohl, Z. Simon, A. Vlad, G. Kaufmann and K. Ponsold, *Z. Naturforsch.*, **1987**, *42c*, 935.
96. I. Gergen, M. Bohl, H. Simon and Z. Simon, *Rev. Roum. Chim.*, **1989**, *34*, 995.
97. Z. Simon and M. Bohl, *Quant. Struct. Act. Relat.*, **1992**, *11*, 23.
98. V. Popoviciu, S. Holban, I. I. Badilescu and Z. Simon, *Studia Biophys (Berlin)*, **1978**, *69*, 75.
99. Z. Simon, G. I. Mihalas and E. Caspi, *Rev. Roum. Chim.*, **1984**, *29*, 83.
100. M. Bohl, Z. Simon and M. Lochmann, *Z. Naturforsch*, **1989**, *44c*, 217.
101. T. I. Oprea, D. Ciubotariu, T. Sulea, and Z. Simon, *Quant. Struct. Act. Relat.*, **1993**, *12*, 21.
102. R. D. Cramer, III, D. E. Patterson and J. D. Bunce, *J. Amer. Chem. Soc.*, **1986**, *110*, 5959.
103. Maria Mracec, S. Muresan, M. Mracec, Z. Simon and G. Naray-Szabo, *Quant. Struct. Act. Relat.*, **1997**, *16*, 459.
104. Maria Mracec, M. Mracec, C. Bologa and Z. Simon, *SAR and QSAR in Envir. Res.*, **2001**, *12*, 143.
105. Maria Mracec, M. Mracec, L. Kurunczi, T. Nusser and Z. Simon, *J. Molec. Struct (Theochem)*, **1996**, *36*, 139.
106. Maria Mracec, M. Mracec, C. Bologa and Z. Simon, *Annals West Univ. Timişoara, Ser. Chem.*, **1998**, *7*, 155.
107. Maria Mracec, Otilia Costisor, Liliana Cseh, M. Mracec and Z. Simon, *Rev. Roum. Chim.*, **2004**, *49*, 199.
108. C. Mihart, A. Chiriac, Veronica Chiriac and Z. Simon, *Preprint Univ. Timişoara Ser. Chim.*, **1981**, no. 5.
109. Z. Simon and A. Chiriac, *Preprint Univ. Timişoara Ser. Chim.*, **1985**, no. 9.
110. Z. Simon and A. Chiriac, *Preprint Univ. Timişoara Ser. Chim.*, **1985**, no. 10.
111. S. Timofei, L. Kurunczi, "Aplicarea relaţiilor de tip QSAR la studiul adsorbţiei coloranţilor pe celuloză", "Relaţii cantitative structură chimică-activitate biologică (QSAR). Metoda MTD", A. Chiriac, D. Ciubotariu and Z. Simon, (coord.), Ed. Mirton, Timişoara, 1996, p. 205-220 (ISBN 973-578-140-9).
112. S. Funar-Timofei, A. Salló, G. Simu, L. Kurunczi, "Structure-Affinity Relations in the Dye-Fibre Interactions", "Quantum Biochemistry and Specific Interactions", (A. Chiriac, M. Mracec, T.I. Oprea, L. Kurunczi, Z. Simon, Eds.), Ed. Mirton, Timişoara, 2002, ISBN: 973-585-805-3, p. 220-232.
113. S. Funar-Timofei, A. Sallo, G. Simu, L. Kurunczi, "Structure Affinity Relations in Dye-Fibre Interactions", "Quantum Biochemistry and Specific Interactions", Second Edition, A. Chiriac, M. Mracec, T.I. Oprea, L. Kurunczi, Z. Simon (Eds.), Mirton Publishing House, Timişoara, 2003, p. 225-237.
114. S. Timofei, Z. Simon, W. Schmidt, L. Kurunczi, "Tendinţe şi proprietăţi în sinteză şi aplicarea coloranţilor, Zilele Academice Ieşene", Roumania, 5–7 Nov., 1992, p. 119-122.
115. S. Timofei, W. Schmidt, L. Kurunczi, Z. Simon, A. Sallo, *Dyes Pigments,* **1994**, *24*:, 267-279.
116. S. Timofei, L. Kurunczi, W. Schmidt, W.M.F. Fabian, Z. Simon, *Quant. Struct.–Act. Relat.,* **1995**, *14*, 444-449.
117. W.M.F. Fabian, S. Timofei, L. Kurunczi, *J. Mol. Struct., THEOCHEM* **1995**, *340*, 73-81.
118. S. Timofei, L. Kurunczi, W. Schmidt, Z. Simon, *Rev. Roum. Chim.,* **1997**, *42*, 687-692.
119. S. Timofei, L. Kurunczi, W. Schmidt, Z. Simon, *Dyes Pigments,* **1996**, *32*, 25-42.
120. S. Funar-Timofei, G. Schüürmann, *J. Chem. Inf. Comput. Sci*., **2002**, *42*, 788-795
121. G. Schüürmann, S. Funar-Timofei, *J. Chem. Inf. Comput. Sci*., **2003**, *43*, 1502-1515.
122. S. Timofei, L. Kurunczi, Z. Simon, *MATCH-Commun. Math. Co.*, **2001**, *44*, 349-360.
123. S. Timofei, L. Kurunczi, Z. Simon, *Annals of West University of Timişoara, ser. Chem.*, **2001**, *10* , 1031-1040.
124. S. Timofei, W.M.F. Fabian, *J. Chem. Inf. Comput. Sci.* **1998**, *38*, 1218-1222.
125. W.M.F. Fabian, S. Timofei, *J. Mol. Struct., THEOCHEM* **1996**, *362*, 155 –162.
126. S. Timofei, L. Kurunczi, W. Schmidt, Z. Simon, *Dyes Pigments* **1995**, *29*, 251-258.
127. T.I. Oprea, L. Kurunczi, S. Timofei, *Dyes Pigments* **1997**, *33*, 41-64.
128. S. Timofei, W. Schmidt, L. Kurunczi, Z. Simon, *Dyes Pigments*, **2000**, *47*, 5-16.
129. S. Timofei, L. Kurunczi, *Annals of West University of Timişoara, ser. Chem.*, **2000**, *9*, 219-226.

130. S. Timofei, L. Kurunczi, Z. Simon, *Annals of West University of Timişoara, ser. Chem.*, **2000**, *9*, 227-234.
131. S. Timofei, L. Kurunczi, S. Iliescu, *Annals of West University of Timişoara, ser. Chem.*, **2001**, *10*, 937-942.
132. L. Kurunczi, S. Timofei, S. Iliescu, *Phosphorus, Sulfur and Silicon*, **2002**, *177*, 1713-1716.
133. S. Timofei, L. Kurunczi, S. Iliescu, *Chem. Bull. „POLITEHNICA" Univ. Timişoara*, **2001**, *46*, 1-2, 231-236.
134. R. Kaliszan, *J. Chromatog. B*, **1998**, *715*, 229–244.
135. S. Funar-Timofei, T. Suzuki, J. A. Paier, A. Steinreiber, K. Faber, W. M. F. Fabian, *J. Chem. Inf. Comput. Sci*., **2003**, *43*, 934-940.
136. T. Suzuki, S. Timofei, B. E. Iuoras, G. Uray, P. Verdino, W. M. F. Fabian, *J. Chromatogr. A.*, **2001**, *922*, 13-23.
137. S. Timofei, *Annals of West University of Timişoara, ser. Chem.*, **2001**, *10*, 841-856.
138. G. Simu, S. Timofei, E. Sarandan, *Annals of West University of Timişoara, ser. Chem.*, **2001**, *10*, 857-862.
139. S. Funar-Timofei, G. Simu, E. Sărăndan, *Sutdia Univ. "Babeş-Bolyai", CHEMIA,* **2002**, *47*, 83-93.
140. G. M. Simu, S. Funar-Timofei, E. Sărăndan, *Rev.Chim.-Bucharest*, **2003**, *7*, 603-607.
141. S. Funar-Timofei, E. Sărăndan, A. Salló, F. Eleneş, E. Crăşmăreanu, *Rev.Chim.(Bucharest)*, **2003**, *10*, 802-806.
142. S. Funar-Timofei, L. Kurunczi, A. Sallo, E. Sărăndan, F. Eleneş, E. Crăşmăreanu, Z. Simon, *Annals of West University of Timişoara, ser. Chem.*, **2003**, *12*, 153-162.
143. E. Şeclăman, A. Salló, F. Eleneş, C. Crăşmăreanu, C. Wikete, S. Timofei, Z. Simon, *Dyes Pigments*, **2002**, *55*, 69-77.
144. T. Suzuki, S. Timofei, L. Kurunczi, U. Dietze, G. Schüürmann, *Chemosphere*, **2001**, *45*, 1-9.